Topological Insulators in Ternary Compounds with a Honeycomb Lattice

Hai-Jun Zhang,[1] Stanislav Chadov,[2] Lukas Müchler,[1,2] Binghai Yan,[1] Xiao-Liang Qi,[1] Jürgen Kübler,[3] Shou-Cheng Zhang,[1] and Claudia Felser[1,2,*]

[1]*Department of Physics, McCullough Building, Stanford University, Stanford, California 94305-404531, USA*
[2]*Institut für Anorganische Chemie und Analytische Chemie, Johannes Gutenberg - Universtität, 55099 Mainz, Germany*
[3]*Institut für Festkörperphysik, Technische Universität Darmstadt, 64289 Darmstadt, Germany*

(Received 11 October 2010; published 11 April 2011)

We investigate a new class of ternary materials such as LiAuSe and KHgSb with a honeycomb structure in Au-Se and Hg-Sb layers. We demonstrate the band inversion in these materials similar to HgTe, which is a strong precondition for existence of the topological surface states. In contrast with graphene, these materials exhibit strong spin-orbit coupling and a small direct band gap at the Γ point. Since these materials are centrosymmetric, it is straightforward to determine the parity of their wave functions, and hence their topological character. Surprisingly, the compound with strong spin-orbit coupling (KHgSb) is trivial, whereas LiAuSe is found to be a topological insulator.

DOI: 10.1103/PhysRevLett.106.156402 PACS numbers: 71.20.−b, 73.20.−r, 73.43.−f

The discovery of two- and three-dimensional topological insulating (TI) materials has generated great interest within the condensed matter physics community [1–4]. A 2D TI with quantum spin-Hall effect was predicted and observed in the binary semiconductor HgTe [5,6]. In a series of single crystals, such as Bi_2Se_3, 3D TI behavior was observed in surface states appearing as Dirac cones [7–9]. The TI properties in these materials can be understood from a simple mechanism of band inversion (BI) caused by spin-orbit coupling (SOC). Later on, the manifold of Heusler semiconductors with 18 valence electrons and a similar BI was proposed [10,11]. Since the Heusler class is extremely rich, it provides much wider flexibility in design by tuning the band gap and the SOC. In addition, the multifunctionality allows the incorporation of new properties such as superconductivity or magnetism [10]. The structure of the *XYZ* Heusler compounds can be viewed as ''stuffed'' *YZ* zinc blende. Depending on the stuffing element *X* they are semiconducting or semimetallic [12]. Heusler materials like ScPtBi are topologically similar to HgTe: the BI occurs due to small electronegativity differences.

In this Letter we propose a new class of TIs which are structurally related to Heuslers. As mentioned above Heusler compounds can be viewed as stuffed diamond. Analogously, the honeycomb structure with 18 valence electrons can be obtained by stuffing the graphite lattice [13]. Thus it might be possible to find among them heavy compounds with inverted band structure. Indeed, KHgSb and LiAuSe, for example, exhibit band ordering similar to the cubic HgTe. Moreover, in contrast to graphene [14] the strong SOC in these compounds leads to a finite band gap at the Γ point. Therefore, these structures might realize the 3D TI behavior.

For instance, KHgSb, which has the ZrBeSi lattice (also called AlB_2 or Ni_2In lattice), can be presented as stuffed graphene: the electropositive K^+ is stuffed into the honeycomb lattice of $[HgSb]^-$ [13]. Such ZrBeSi structure with additional stuffing electropositive main group elements is illustrated in Fig. 1: the main group and the transition elements alternate within the same layer and between the layers; therefore, the primitive unit cell consists of two formula units. Since they are centrosymmetric, the determination of the wave function parity at the time-reversal symmetric (TRS) points for these materials is possible.

The number of ternary compounds of this structure is nearly as large as in the Heusler family; however, due to weaker mean hybridization (sp^2 versus sp^3) many of the 18 valence electron compounds exhibit substantially smaller gaps or are simply metallic. In contrast to HgTe and ScPtBi, such materials with inverted structure exhibit real band gaps due to their higher structural anisotropy. For this reason the honeycomb compounds are 3D, rather than 2D, TIs. The 3D TIs exhibit an insulating energy gap in the bulk and gapless states on the surface protected by TRS [15]. This holds only if there is an odd number of massless Dirac cones (single cone in the simplest case). The oddness is provided by the Z_2 topological invariant of the bulk [16,17]; thus, any TRS perturbation cannot open an insulating gap at the Dirac point on the surface.

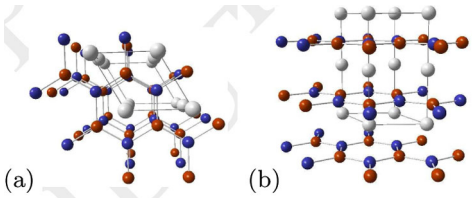

FIG. 1 (color online). The lattice of honeycomb compound *XYZ* (the ZrBeSi structure type) shown in (a) the *ab* plane and (b) the *ac* plane. Thus, the ternary semiconductor (with 18 valence electrons) can be viewed as *X* stuffed (*X* = Li, Na, K) graphene *YZ* lattice consisting of alternating late transition metals *Y* (Ag, Au, Zn, Hg) and main group elements *Z* (Se, Te, P, As, Sb).

The bulk band gap depends on the interplay of the lattice constant, SOC, and the electronegativities of the honeycomb sublattice constituents. In analogy to a ternary cubic semiconductors, new TIs can be found among the heavy 8/18 valence electron relatives of graphene, i.e., in a graphite XYZ structure type. Suitable atomic combinations are (i) X = Li, Na, K, Rb, Cs, Y = Zn, Cd, Hg, and Z = P, As, Sb, Bi, (ii) X = K, Rb, Cs, Y = Ag, Au, and Z = Se, Te, or (iii) X = rare earth, Y = Ni, Pd, Pt, and Z = P, As, Sb, Bi. Some of these combinations are not yet synthesized, some crystallize in different forms such as variants of the Cu_2Sb structure type, and some, especially the rare earth containing compounds, are metallic. The known examples are KZnAs, KZnSb, KZnP, KHgAs, KHgSb, RbZnP, RbZnAs, RbZnSb, NaAuTe, KCuSe, KCuTe, KAuTe, and RbAuTe. Compounds such as LiAuSe, LiAuTe, CsAuTe, KHgBi, and CsHgBi are likely to be synthesized and we consider them in the present study as well. As mentioned above, the electronic structure of these materials is similar to their cubic analogues. The alkaline ions Li^+, Na^+, K^+, Rb^+, and Cs^+ "stuff" the graphite-type YZ planar sublattice. Since these 18-electron compounds form closed-shell structures, they are all nonmagnetic and semiconducting. The difference is that in the case of binary semiconductors or C_{1b} Heuslers, the bonds within the YZ tetrahedrons are of sp^3 or sd^3 type, whereas in planar graphite-type layers the σ-type bonding occurs between the sp^2 or sd^2 orbitals. The remaining p orbitals provide the π-type bonding interaction, similar to graphite.

The search for the topological character of the proposed materials is based on density functional *ab initio* electronic structure calculations [18,19] (see the supplemental material [20]). The important peculiarity of hexagonal systems is emphasized here: their unit cell consists of two formula units which results in a doubling of the corresponding bands. More details are given in the supplemental material ([20], Fig. 1) where it is seen that for KZnP (KHgSb) the doubled s bands at the Γ point are split by about 10 meV. Thus, for the weak coupling of the nearest honeycomb planes, these doubled bands can become nearly indistinguishable. In the following we show that such doubling of the unit cell leads to a change of topology. Fortunately, the centrosymmetric space group (no. 194) of the honeycomb compounds allows us to make use of the parity eigenvalues [21]. All relevant properties, i.e., the wave function parity in TRS k points, the Z_2 invariant, the average nuclear charge $\langle Z \rangle$, the band gap width E_g at the Γ point, and corresponding lattice parameters, are listed in Table I for the compounds studied here.

From previous studies on binary and ternary cubic semiconductors [10] it follows that it is more probable to find the $Z_2 = 1$ TI among heavier compounds (with stronger

TABLE I. Calculated parities at the TRS points, Z_2 topological invariant [21], average nuclear charge per unit cell $\langle Z \rangle$, band gap width E_g at the Γ point, and lattice parameters. Note, that all XYZ, Z = P, compounds are found trivial and therefore are not listed.

	Γ	M	L	A	Z_2	$\langle Z \rangle$	E_g (meV)	a [a.u.]	c/a
LiAgSe	+	−	−	−	1	28	1	8.507	1.512
LiAgTe	−	−	−	−	0	34	45	8.979	1.526
LiAuSe	+	−	−	−	1	38.(6)	50	8.353	1.670
LiAuTe	+	−	−	−	1	44.(6)	⋯	8.818	1.663
NaAgSe	+	−	+	+	1	30.(6)	10	8.544	1.737
NaAgTe	+	−	+	+	1	36.(6)	3	9.031	1.719
NaAuSe	+	−	+	+	1	41.(3)	15	8.427	1.855
NaAuTe	+	−	+	+	1	47.(3)	30	8.894	1.823
KAgSe	−	−	+	+	0	33.(3)	15	8.836	1.989
KAgTe	−	−	+	+	0	39.(3)	230	9.193	1.958
KAuSe	−	−	+	+	0	44	20	8.742	2.077
KAuTe	+	−	+	+	1	50	⋯	8.780	2.097
LiZnAs	−	−	−	−	0	22	280	7.881	1.791
LiZnSb	−	−	−	−	0	28	10	14.121	1.762
LiHgAs	+	−	−	−	1	38.(6)	⋯	8.542	1.686
LiHgSb	+	−	−	−	1	44.(6)	⋯	9.070	1.665
NaZnAs	−	−	+	+	0	24.(6)	80	7.952	2.083
NaZnSb	−	−	+	+	0	30.(6)	230	8.539	2.007
NaHgAs	−	−	+	+	0	41.(3)	⋯	8.615	1.897
NaHgSb	−	−	+	+	0	47.(3)	140	9.148	1.845
KZnAs	−	−	+	+	0	27.(3)	160	7.993	2.419
KZnSb	−	−	+	+	0	33.(3)	130	8.654	2.349
KHgAs	−	−	+	+	0	44	80	8.515	2.214
KHgSb	−	−	+	+	0	50	250	9.040	2.140

SOC). Indeed, their band splitting scales roughly with the average nuclear charge $\langle Z\rangle = 1/N\sum_{i=1}^{N} Z_i$, where $N = 2$ for binaries and $N = 3$ for ternaries. This parameter sorts cubic systems almost in a straight line [10]. However, Table I clearly illustrates that this does not hold for the ZrBeSi structure type. Indeed, only lithium compounds within the Zn and Hg group show the expected trend. The compounds with Zn are topologically trivial, whereas those with Hg are nontrivial insulators. Compounds with heavier alkaline metals (Na, K) are all trivial independently of whether or not they contain Zn or Hg. Among the Ag- and Au-containing compounds, more nontrivial systems are found; however, the correlation between the BI and $\langle Z\rangle$ as in the cubic semiconductors, is absent. For example, the TI LiAgSe corresponds to $\langle Z\rangle = 28$, whereas for the topologically trivial KHgSb system $\langle Z\rangle = 50$.

In Fig. 2 the band structure of LiAuSe (upper panel) is compared with KHgSb (lower panel) calculated at TRS points with (right) and without (left) SOC. It follows that both compounds are semimetals with degeneracies at the Γ and A symmetry points if SOC is omitted. The degenerate p_x and p_y states mediate σ-type Sb/Se and Hg/Au bonding. The lower-lying Hg/Au bands are of s type, similar to HgTe. Inclusion of SOC opens a band gap at E_F at the Γ and A points leading to typical dips in the band structure for both compounds. The resulting parities for both materials listed in Table I match only at the M point, whereas at Γ, A, and L they differ, leading to a topologically trivial state in KHgSb and nontrivial in LiAuSe. It should be noted that in LiAuSe occurs the band crossing at E_F along the Γ-A direction due to the threefold rotational symmetry. By breaking it, i.e., by applying small in-plain strain in the [110] direction, the band gap could be opened by keeping the topologically nontrivial state of the system [see Figs. 4(c) and 4(d)].

To understand the mechanisms of the BI and parity change in detail, one can track the band structure evolution near the Γ point by starting from simple atomic energy levels and subsequently introducing chemical bonding (step I), crystal field splitting (II), and SOC (III). KZnP, LiAuSe, and KHgSb are taken as examples and schematically shown in Figs. 3(a)–3(c). KZnP shows no BI with Zn s above the P p orbitals, similar to CdTe. LiAuSe and KHgSb are different. Since Au (or Hg)-d shell is very delocalized, Au (Hg) s is pulled down below Se (Sb) p, which leads to the first BI as shown in step I of Figs. 3(b) and 3(c), similar to the HgTe case [22]. On one hand, LiAuSe has moderate SOC strength and no further BI happens when introducing SOC in step III [Fig. 3(b)]. Therefore, we conclude that LiAuSe is topologically nontrivial with a single BI. On the other hand, KHgSb exhibit such strong SOC that the second BI occurs in step III [Fig. 3(c)]. Double BI means double parity exchange, which makes KHgSb a trivial material. In order to show this more clearly, a scheme of the band structures at Γ point is given for KZnP, LiAuSe, and KHgSb in Figs. 3(d)–3(f).

Since the evident manifestation of the TI is the presence of the an odd number of Dirac cones at the surface, in the following we calculate it explicitly by constructing the tight-binding (TB) Hamiltonian for the semi-infinite system with (0001) surface on the basis of the maximally localized Wannier functions (MLWF) [23,24] approach for

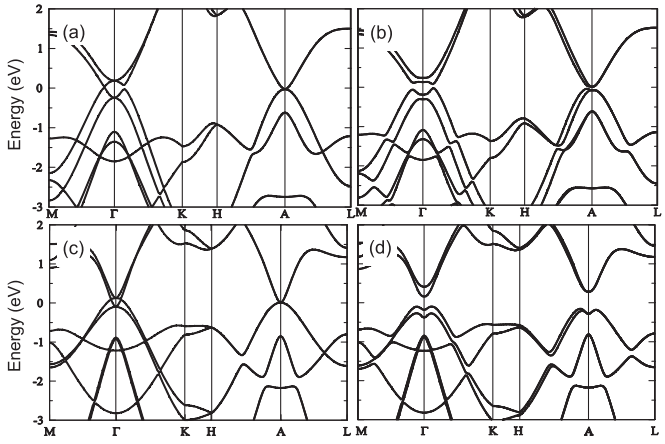

FIG. 2. Band structure of LiAuSe (a),(b) and KHgSb (c),(d) calculated without (a),(c) and with (b),(d) SOC.

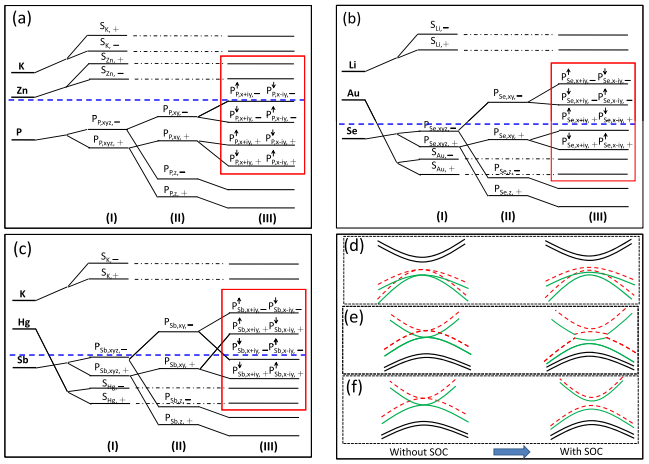

FIG. 3 (color online). Evolution of the band structure at the Γ point starting from atomic orbitals for KZnP (a). The chemical bonding is introduced in step I. In step II the crystal field is switched on. These $p_{x,y,z}$ orbitals split into $p_{x,y}$ and p_z due to the hexagonal symmetry. Then SOC is turned on in step III. This splits the energy levels further. "↑↓" represents spin labels. The parity labels "±"are also shown. The blue dashed line marks the E_F. One notices that the Zn s bands are above the P p bands for KZnP. Similarly, the schemes of LiAuSe and KHgSb are shown in (b) and (c), respectively. The main difference to KZnP is that the Au (or Hg) s orbital and the Se (or Sb) p orbital are inverted. KHgSb has a second BI in step III, while LiAuSe does not. Panels (d)–(f) show the schematic band structure for KZnP, LiAuSe, and KHgSb near Γ, respectively. The black curves mark the s bands. Gray dashed (red) and gray solid (green) lines stand for the p bands with "−" and "+" parities, respectively.

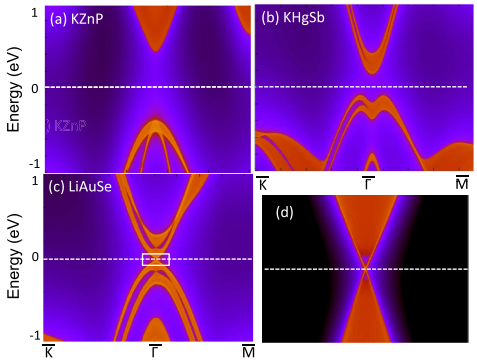

FIG. 4 (color online). Surface states of semi-infinite (0001) surfaces corresponding to topologically trivial (a) KZnP, (b) KHgSb, and nontrivial (c) LiAuSe insulators (strained case) calculated along $\bar{K}$-$\bar{\Gamma}$-$\bar{M}$ in the Brillouin zone. In contrast to KZnP and KHgSb, LiAuSe exhibits the surface states seen in the bulk energy gap, zoomed in the inset (d).

three particular examples discussed in Fig. 3. To simplify the calculations, the MLWF hopping parameters are derived from the bulk *ab initio* calculations (without surface corrections). Using this TB model we apply the iterative method [25] to obtain the surface Green function. The corresponding Bloch spectral functions for KZnP, KHgSb, and LiAuSe are plotted in Fig. 4. The bulk and the surface states show up very clearly. In agreement with the scheme outlined in Fig. 3, KZnP and KHgSb remain insulators at the surface and only LiAuSe exhibits gapless surface states seen as a single cone within the bulk energy gap at the Γ point. The semi-infinite LiAuSe system with the Li and Au-Se terminations shows almost the same surface states. An estimate of its Fermi velocity gives 1.8×10^5 m/s, which is smaller than that for Bi_2Se_3. Thus the surface calculation agrees with the bulk parity analysis and undoubtedly confirms the existence of the topologically nontrivial materials within proposed honeycomb structure. The MLWF TB approach without the surface correction is reasonable because these surface states originate from the topological nature of its bulk system only. Though the details of the surface corrections cannot destroy the topological surface states, they still can contribute some trivial surface states from, e.g., the dangling bonds. The additional *ab initio* calculations of the freestanding slabs confirm the existence of nontrivial surface states as well (see the supplemental material [20]).

In conclusion, we have shown that topologically nontrivial systems can be found in the class of honeycomb structure semiconductors. The interplay of mechanisms responsible for the trivial or nontrivial character in these systems, however, differs from the cubic semiconductors studied earlier. In particular, it is emphasized that the strong SOC and weak interlayer coupling causes a double BI which in turn makes the compound trivial.

The authors thank X. Q. Chen for valuable discussion. The work was supported by the supercomputing center at Stanford Institute Materials and Energy Science. The financial support of the DFG/ASPIMATT project (unit 1.2-A) and the Army Research Office (No. W911NF-09-1-0508) is gratefully acknowledged.

*felser@uni-mainz.de

[1] X. Qi and S. Zhang, Phys. Today **63**, No. 1, 33 (2010).
[2] M. Z. Hasan and C. L. Kane, Rev. Mod. Phys. **82**, 3045 (2010).
[3] J. Moore, Nature (London) **464**, 194 (2010).
[4] X. Qi and S. Zhang, arXiv:1008.2026.
[5] B. A. Bernevig, T. L. Hughes, and S. C. Zhang, Science **314**, 1757 (2006).
[6] M. König, S. Wiedmann, C. Brüne, A. Roth, H. Buhmann, L. Molenkamp, X.-L. Qi, and S.-C. Zhang, Science **318**, 766 (2007).
[7] H. Zhang, C.-X. Liu, X.-L. Qi, X. Dai, Z. Fang, and S.-C. Zhang, Nature Phys. **5**, 438 (2009).
[8] Y. Xia, D. Qian, D. Hsieh, L. Wray, A. Pal, H. Lin, A. Bansil, D. Grauer, Y. S. Hor, R. J. Cava, and M. Z. Hasan, Nature Phys. **5**, 398 (2009).
[9] Y. L. Chen, J. G. Analytis, J.-H. Chu, Z. K. Liu, S.-K. Mo, X. L. Qi, H. J. Zhang, D. H. Lu, X. Dai, Z. Fang, S. C. Zhang, I. R. Fisher, Z. Hussain, and Z.-X. Shen, Science **325**, 178 (2009).
[10] S. Chadov, X. L. Qi, J. Kübler, G. H. Fecher, C. Felser, and S. C. Zhang, Nature Mater. **9**, 541 (2010).
[11] H. Lin, L. A. Wray, Y. Xia, S. Xu, S. Jia, R. J. Cava, A. Bansil, and M. Z. Hasan, Nature Mater. **9**, 546 (2010).
[12] H. C. Kandpal, C. Felser, and R. Seshadri, J. Phys. D **39**, 776 (2006).
[13] F. Casper, C. Felser, R. Seshardi, P. Sebastian, and R. Pöttgen, J. Phys. D **41**, 035002 (2008).
[14] B. A. Bernevig and S. C. Zhang, Phys. Rev. Lett. **96**, 106802 (2006).
[15] L. Fu, C. L. Kane, and E. J. Mele, Phys. Rev. Lett. **98**, 106803 (2007).
[16] C. L. Kane and E. J. Mele, Phys. Rev. Lett. **95**, 226801 (2005).
[17] C. L. Kane and E. J. Mele, Phys. Rev. Lett. **95**, 146802 (2005).
[18] W. Kohn and L. J. Sham, Phys. Rev. **140**, A1133 (1965).
[19] P. Hohenberg and W. Kohn, Phys. Rev. **136**, B864 (1964).
[20] See supplemental material at http://link.aps.org/supplemental/10.1103/PhysRevLett.106.156402 for details of electronic structure calculation (including surface and slab), parity definition, and illustration of the analogy in the band structures of cubic and hexagonal semiconductors.
[21] L. Fu and C. L. Kane, Phys. Rev. B **76**, 045302 (2007).
[22] A. Delin, Phys. Rev. B **65**, 153205 (2002).
[23] N. Marzari and D. Vanderbilt, Phys. Rev. B **56**, 12 847 (1997).
[24] I. Souza, N. Marzari, and D. Vanderbilt, Phys. Rev. B **65**, 035109 (2001).
[25] M. P. L. Sancho, J. M. L. Sancho, J. M. L. Sancho, and J. Rubio, J. Phys. F **15**, 851 (1985).